



Delft University of Technology

## Effect of resin-rich bond line thickness and fibre migration on the toughness of unidirectional Carbon/PEEK joints

Sacchetti, Francisco; Grouve, Wouter J B; Warnet, Laurent L.; Villegas, Irene Fernandez

**DOI**

[10.1016/j.compositesa.2018.02.035](https://doi.org/10.1016/j.compositesa.2018.02.035)

**Publication date**

2018

**Document Version**

Accepted author manuscript

**Published in**

Composites Part A: Applied Science and Manufacturing

**Citation (APA)**

Sacchetti, F., Grouve, W. J. B., Warnet, L. L., & Villegas, I. F. (2018). Effect of resin-rich bond line thickness and fibre migration on the toughness of unidirectional Carbon/PEEK joints. *Composites Part A: Applied Science and Manufacturing*, 109, 197-206. <https://doi.org/10.1016/j.compositesa.2018.02.035>

**Important note**

To cite this publication, please use the final published version (if applicable).

Please check the document version above.

**Copyright**

Other than for strictly personal use, it is not permitted to download, forward or distribute the text or part of it, without the consent of the author(s) and/or copyright holder(s), unless the work is under an open content license such as Creative Commons.

**Takedown policy**

Please contact us and provide details if you believe this document breaches copyrights.

We will remove access to the work immediately and investigate your claim.

1   **Effect of resin-rich bond line thickness and fibre migration on the**  
2   **toughness of unidirectional Carbon/PEEK joints**

3   Francisco Sacchetti<sup>1,2</sup>, Wouter J.B. Grouve<sup>1</sup>, Laurent L. Warnet<sup>2</sup>, Irene  
4   Fernandez Villegas<sup>3</sup>

5   <sup>1</sup>*ThermoPlastic composites Research Center (TPRC), Enschede, The Netherlands*

6   <sup>2</sup>*Faculty of Engineering Technology, Chair of Production Technology, University of Twente,*  
7   *Enschede, The Netherlands*

8   <sup>3</sup>*Structural Integrity and Composites, Faculty of Aerospace Engineering, Delft University of*  
9   *Technology, Delft, The Netherlands*

10   Palatijn 15, P.O. Box 770, 7500AE Enschede, The Netherlands

11   Email: Laurent Warnet ([email to:l.warnet@utwente.nl](mailto:l.warnet@utwente.nl)), web page: <http://www.tprc.nl>

12

13      **Effect of resin-rich bond line thickness and fibre migration on the**  
14      **toughness of unidirectional Carbon/PEEK joints**

15            *Abstract*

16        *It is a common practice in fusion bonding of thermoplastic composites to add a matrix*  
17        *layer between the two substrates to be joined. The aim is to ensure proper wetting of*  
18        *the two parts. The effect of this additional matrix layer on the mechanical performance*  
19        *was studied by mode I fracture toughness measurements. The additional matrix was*  
20        *inserted at the interface in the form of films of various thicknesses. Three different*  
21        *manufacturing techniques, namely autoclave consolidation, press consolidation and*  
22        *stamp forming, were used to prepare different sets of specimens with varying resin-rich*  
23        *bond line thickness. The occurrence of fibre migration towards the matrix rich*  
24        *interface was induced by the manufacturing techniques used due to their different*  
25        *processing times. The interlaminar fracture toughness was observed to increase with*  
26        *increasing amount of extra-matrix at the interface, while no effects of the fibre*  
27        *migration on the fracture toughness were observed.*

28      Keywords: thermoplastic composites, fusion bonding, matrix interleaving, fracture mechanics,  
29      fractography

30

31    **1. Introduction**

32    Fusion bonding can be considered as an affordable way to assemble thermoplastic composite  
33    parts [1]. From a practical viewpoint, the process involves heating of the interface between  
34    the parts, followed by the application of pressure and cooling down. There are many fusion  
35    bonding techniques available, all differing in the way heat and pressure are applied to the  
36    interface [2, 3]. Two groups of fusion bonding techniques can be distinguished by the size of  
37    the area heated, namely bulk heating and welding, which is characterised by local heating.  
38    The first group consists of bringing the entire part to melt and using the tooling to maintain  
39    pressure throughout the process. Consequently, this technique is characterised by a relatively  
40    long processing time (1-2 hours) [4]. The second group is characterised by local heating, and  
41    sometimes by local application of pressure, which means that a short processing time can be  
42    achieved (minutes or seconds).

43    From a physical viewpoint, the fusion bonding process involves intimate contact  
44    development between the two surfaces (also known as wetting), followed by interdiffusion of  
45    polymer chains across the interface (also known as healing) [5]. Proper wetting may be a  
46    challenge for thermoplastic composites with a high fibre volume fraction due to the lack of  
47    matrix material at the interface; this may result in poor bond performance [6]. To solve this  
48    problem, an additional layer of neat polymer can be inserted (interleave) at the interface in  
49    order to promote wetting [7, 8, 9]. Moreover, some welding techniques may, in any case,  
50    require such an additional resin layer at the interface. For example, a resin layer is added as  
51    an energy director in the case of ultrasonic welding, while resistance welding requires a metal  
52    mesh embedded in a matrix layer at the interface [5, 10]. This additional layer of pure  
53    polymer may lead to a matrix rich bond line which in turn may affect the joint performance.  
54    A proper understanding of the interrelation between the matrix rich bond line thickness and  
55    the joint performance is required to enable optimisation of the joint design.

58 Earlier research showed that the interlaminar fracture toughness of Carbon/PEEK increases  
59 with interleaving thickness (i.e. with increasing thickness of the matrix rich bond line) [11,  
60 9]. This is in line with the work on other material systems [12, 13, 14, 15] and adhesives  
61 joints [16, 17] and is generally related to the size of the plastic yielding zone in front of the  
62 crack tip. An increase in matrix interface thickness allows for a larger plastic yielding zone,  
63 resulting in a higher interlaminar fracture toughness. It is proposed that the interlaminar  
64 toughness eventually reaches a plateau value equal to the matrix toughness for larger matrix  
65 interleaved thicknesses [18, 16]. To the best of the authors' knowledge, the aforementioned  
66 studies were all performed on samples manufactured using a typical (bulk heating)  
67 consolidation technique, i.e. either autoclave or press consolidation. These techniques are  
68 characterised by a long processing time, which allows fibres to migrate into the matrix rich  
69 area at the interface. The long processing times are not representative of what happens during  
70 welding. In this case, the short processing times are expected to significantly reduce fibre  
71 migration. It is not clear how this fibre migration affected the measured toughness values  
72 reported in the literature. Two effects may play a role, on one hand, fibre migration leads to  
73 more fibre-fibre contact, which effectively reduces the plastic zone size and, hence, the  
74 fracture toughness [19, 13]. On the other hand, fibre migration may also lead to fibre nesting,  
75 resulting in so-called fibre bridging which causes an increase in toughness [20, 21].  
76 In this research, the effect of interleaving thickness and fibre migration on the interlaminar  
77 fracture toughness of unidirectional carbon fibre reinforced poly-ether-ether-ketone  
78 (Carbon/PEEK) fusion bonded samples was studied. The interleave thickness was varied by  
79 adding unreinforced PEEK films of varying thickness at the interface between the laminates,  
80 while the extent of fibre migration was varied by using different processes. Two slow  
81 processes, autoclave consolidation and press consolidation, and one fast process, stamp

82 forming, were used to prepare interleaved fusion bonded samples. The slow processes are  
83 expected to yield samples with a high degree of fibre migration, while the fast process should  
84 prevent significant fibre migration. A mode I double cantilever beam (DCB) test was used to  
85 evaluate the fracture toughness of the joint under mode I failure. Fractographic analysis of the  
86 samples was performed after mechanical testing to investigate the failure behaviour of the  
87 different samples.

88 **2. Experimental methods**

89 Sample preparation consisted of two steps. First, laminates were press consolidated following  
90 the procedure described below. Second, these laminates were used as substrates for a fusion  
91 bonding step in which two substrates were joined to form a sample. The substrates were  
92 fusion bonded using three processing technologies as described in this section. Subsequently,  
93 the physical state and the interlaminar fracture toughness of the samples was characterised by  
94 cross-sectional microscopy and DCB test respectively. The procedures followed to perform  
95 these measurements are described in the following sub-sections.

96       2.1. Materials and substrate manufacturing

97 Press consolidation was used to prepare unidirectional Carbon/PEEK laminates with a  
98 stacking sequence of [0]<sub>12</sub>. The material was provided by TenCate and is known as Cetex®  
99 TC1200. The fibres used in the prepreg is a T300 JB 3K while the polymer is a Victrex  
100 PEEK 150. The prepreg was stacked in a picture frame mould of 300 by 300 mm<sup>2</sup> and  
101 subsequently consolidated using a static Pinette Emidacau Industries press following the  
102 consolidation cycle suggested by TenCate, which is shown in Figure 1. To ensure deboning  
103 of the laminates from the mould, Marbocote® 227CE, a silicon based semi-permanent mould  
104 release agent was used as a release media. These laminates were then used as the substrates  
105 for the fusion bonding processes.

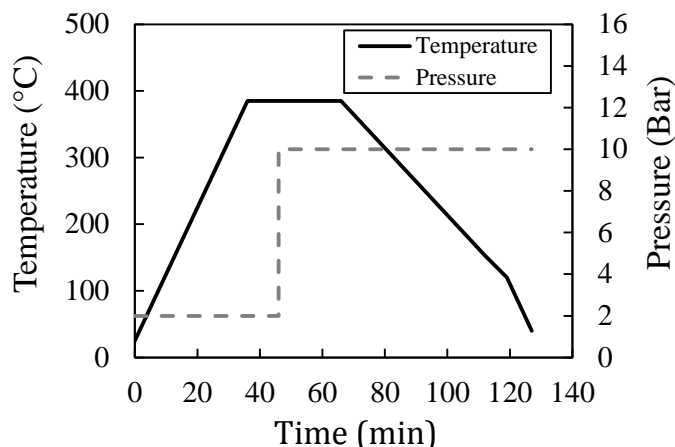


Figure 1: Press cycle used to manufacture the laminates.

## 2.2. Fusion bonding processes

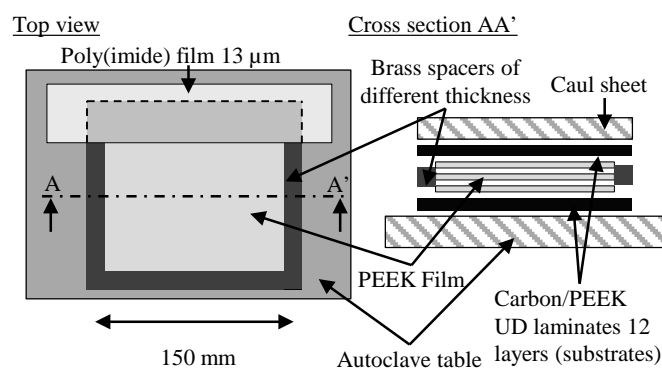
Three different processing techniques were used to prepare the fusion bonded samples, i.e. autoclave consolidation, press consolidation and stamp forming. Regardless of the processing method, a sample was prepared by stacking two substrates on top of each other with optionally additional PEEK film inserted at the interface. The film was manufactured by Victrex and is known under the tradename APTIV®. It was available in two different thicknesses, namely 38 µm and 100 µm. Moreover, a 13 µm thick polyimide film was also inserted between the substrates prior to fusion bonding in order to introduce the pre-crack required for DCB testing. It is worth to notice that in the area where the polyimide film was inserted the additional PEEK films were not inserted. The remainder of this section describes each of the aforementioned processing techniques.

### 2.2.1. Autoclave consolidation

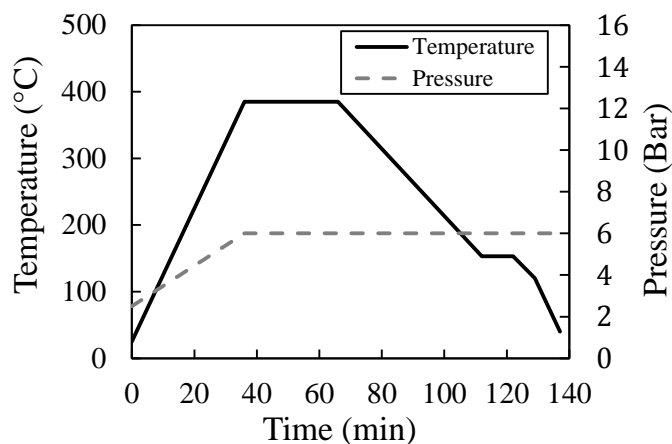
119 An autoclave consolidation process was used to fusion bond the first sample set. Seven  
120 samples were prepared. The first sample was prepared without an additional film at the  
121 interface, while for the other six samples, one to six layers of film with a thickness of 38 $\mu$ m  
122 were inserted at the interface prior to consolidation.

123 A schematic illustration of the autoclave table preparation can be found in Figure 2. The press

124 consolidated substrates were cut into square sections of 150 by 150 mm<sup>2</sup> and subsequently  
125 stacked together with the required film material. Brass picture frames with different  
126 thicknesses were used as a shim at the interface to maintain the distance between substrates  
127 and thereby to prevent the added matrix from being squeezed out. A 10 mm thick aluminium  
128 caul sheet was used to ensure the flatness of the laminate. After wrapping the table in a  
129 vacuum bag, the substrates were fusion bonded in an autoclave at 6 bar pressure and a  
130 temperature of 380 °C based on the process cycle recommended by TenCate, which is shown  
131 in Figure 3.



132 Figure 2: Sketch of the preparation of the autoclave table. In the top view, the upper substrate is not shown for  
133 clarity.  
134



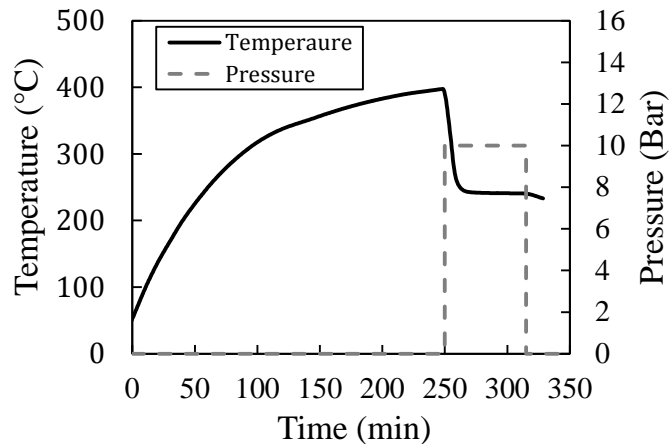
135 Figure 3. Autoclave consolidation cycle used to fusion bond the substrates.  
136  
137  
138  
139  
140

141            2.2.2. *Press consolidation*

142    A second sample set was prepared by press consolidation of two substrates in a press using a  
143    300 by 300 mm<sup>2</sup> picture frame mould. A total of three samples were prepared: one without an  
144    additional polymer film, one with a 38 µm PEEK film and one with a 100 µm PEEK film.  
145    Contrary to the autoclave consolidation process, no shims or spacers were added as any  
146    squeeze flow was restricted by the picture frame mould. The consolidation cycle was the  
147    same as the one used to manufacture the substrates i.e. the cycle as shown in Figure 1.

148            2.2.3. *Stamp forming*

149    The last sample set was prepared by using a Pinette Emidacau Industries stamp forming set  
150    up to fusion bond two substrates. Two substrate laminates were stacked and placed on a  
151    polyimide film of 50 µm thickness, meant for carrying the laminates from the material  
152    loading position to the infrared oven and from the oven to the pressing/stamping position.  
153    The infrared oven was set at a temperature of 450 °C. The substrates were heated up to  
154    complete melting (the temperature at the interface between the two laminates was measured  
155    to be 400 °C, taking around 4 minutes of heating time). Then, the substrates were transferred  
156    to the stamping station where they were fusion bonded and consolidated between two flat  
157    aluminium moulds with a dimension of 250 by 250 mm<sup>2</sup>. The mould temperature was set to  
158    220 °C. The mould halves were quickly closed, and a pressure of 10 bar was applied for 1  
159    minute. The measured temperature and pressure during stamp forming are illustrated in  
160    Figure 4. Three samples were prepared: one without extra polymer, one with a 38 µm PEEK  
161    polymer film and one with a 100 µm PEEK polymer film at the interface between the two  
162    laminates. Table 1 summarises all the samples that were prepared.



163                          Figure 4: Measured temperature and pressure during stamp forming process.

164

Number and thickness ( $\mu\text{m}$ ) of PEEK film plies	Fusion bonding technique/ Sample name		
	Autoclave	Press	Stamp-forming
None	A-None	P-None	S-None
1 x 38 $\mu\text{m}$	A-1x38	P-1x38	S-1x38
2 x 38 $\mu\text{m}$	A-2x38	-	-
1 x 100 $\mu\text{m}$	-	P-1x100	S-1x100
3 x 38 $\mu\text{m}$	A-3x38		
4 x 38 $\mu\text{m}$	A-4x38		
5 x 38 $\mu\text{m}$	A-5x38	-	-
6 x 38 $\mu\text{m}$	A-6x38		

165                          Table 1: Sample description, the thickness of interleaving, and fusion bonding technology used.

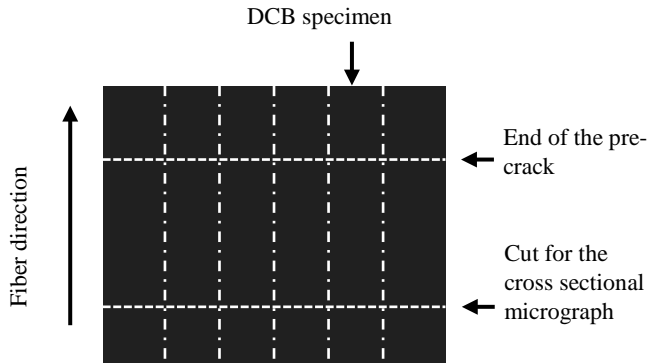
### 166                          2.3. Characterization

167        After fusion bonding, cross-sectional micrographs of the samples were prepared.  
 168        Subsequently, double cantilever beam (DCB) tests were performed followed by a  
 169        fractography analysis.

#### 170                          2.3.1. *Cross-sectional microscopy*

171        The consolidation quality of the fusion bonded samples was characterised using thickness  
 172        measurements and cross-sectional microscopy. The micrographs were taken close to the edge  
 173        of the fusion bonded laminates, while the centre was kept for mechanical testing, as it is  
 174        shown in Figure 5. The microscopy images were also used to evaluate, in a qualitative  
 175        manner, the thickness of the matrix rich bond line and the degree of fibre migration at the

176 interface.



177 Figure 5: Sketch of the location of the cross-sectional sample preparation and the position of the DCB  
178 samples

179 *2.3.2. Double cantilever beam experiments*

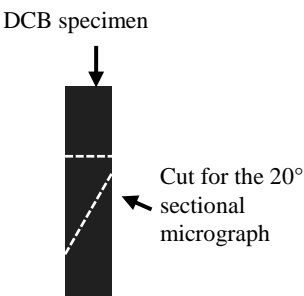
180 The interlaminar fracture toughness of the bond line was evaluated using the double  
181 cantilever beam (DCB) test method. DCB specimens were cut from the fusion bonded  
182 samples in the longitudinal direction of the fibres and then tested according to ISO 15024  
183 [22]. The ISO Standard 15024 is based on the linear elastic fracture mechanics (LEFM). As  
184 such, the conformance of the linear elastic behaviour of the specimens during testing was  
185 evaluated. Figure 5 shows schematically the location of the test specimens cut to a width of  
186 20 mm from the fusion bonded laminates. The specimens were loaded in a servohydraulic  
187 Instron 8500 universal testing machine equipped with a 1 kN force cell. A mode I pre-  
188 cracking procedure was performed for all the specimens according to the standard. The  
189 specimens were loaded at a constant speed of 1.2 mm/min until a delamination crack growth  
190 of about 5 mm has occurred, followed by the specimens unloading until zero force. Next, the  
191 specimens were re-loaded at the same constant speed of 1.2 mm/min until the final  
192 delamination length of about 100 mm has been reached. A travelling recording camera was  
193 used to measure the delamination crack length during testing. The corrected beam theory  
194 (CBT) was used to analyse the data. The interlaminar fracture toughness was calculated as:

$$G_{IC} = \frac{3P\delta}{2w(a + \Delta)} \left( \frac{F}{N} \right), \quad (1)$$

195 where  $P$  is the force,  $\delta$  is the displacement,  $a$  is the crack length,  $w$  is the width of the  
196 specimen,  $F$  is a correction factor for large displacement,  $N$  is a correction factor for the  
197 loading blocks and  $\Delta$  is a correction factor for the rotation of the beam at the crack tip. Since  
198 the delamination length was measured using the horizontal position of the travelling camera  
199 system, there is no need for a large-displacement correction factor ( $F$ ) to be applied to the  
200 measurements [22] (i.e.  $F$  can be considered equal to one). The interlaminar fracture  
201 toughness was calculated both for initiation and propagation. The initiation values were  
202 calculated following the procedure called 5 % / MAX point in the ISO 15024 standard. From  
203 that point on the values measured were considered as propagation values.

204        2.3.3. *Fractography analysis*

205 Two cross-sectional optical micrographs were prepared after testing. One with a sectioning  
206 plane perpendicular to the crack propagation direction and the other with a sectioning plane at  
207  $20^\circ$  with respect to the crack propagation direction. A schematic view of how these cross-  
208 sectional cuts were taken is shown in Figure 6. All the micrographic specimens were  
209 embedded in epoxy and then polished. A Leica DMRX and a Keyence VHX optical  
210 microscope were used to obtain the optical micrographs. Moreover, SEM micrographs of the  
211 fracture surface were made with a Jeol Neoscope JCM-5000. The cross-sectional and  
212 fractography images were analysed in order to determine the crack propagation path and to  
213 identify the main failure modes.



214

Figure 6: Sketch of the location of cross section micrograph cuts for the fractography analysis

215     **3. Experimental results**

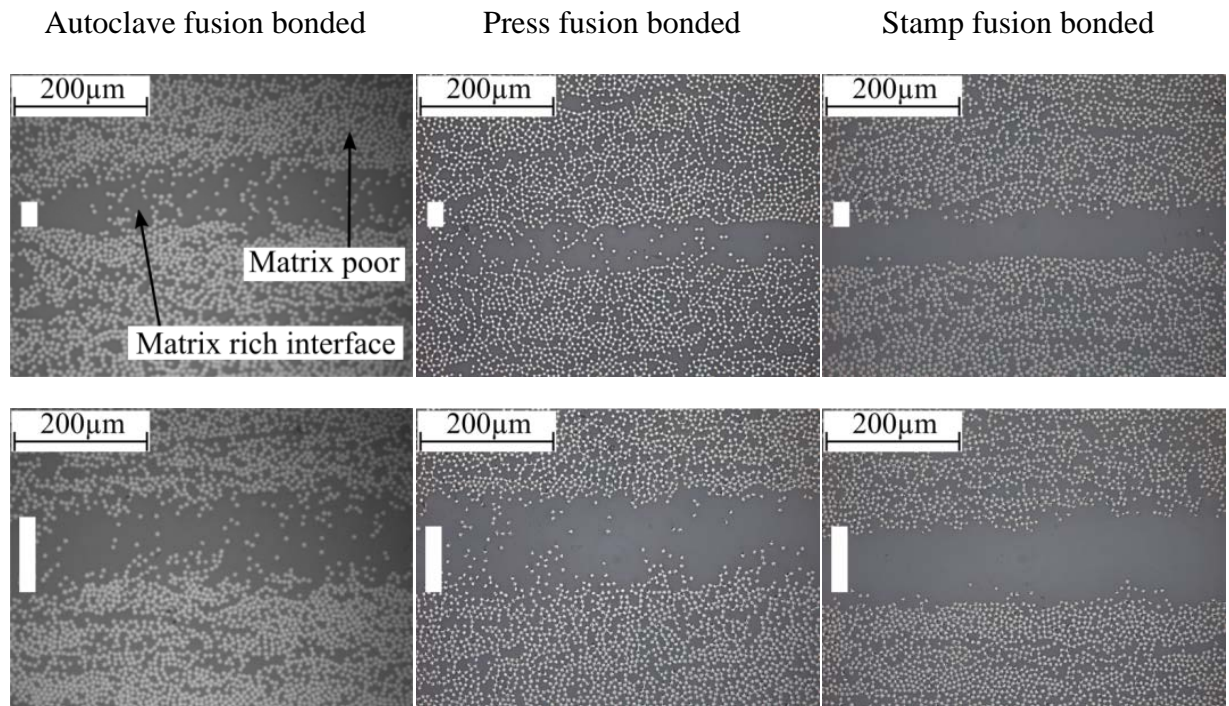
216     The experimental results are elaborated in the present section. First, the physical state of the  
217     samples and bond line microstructure will be evaluated. Subsequently, the fracture toughness  
218     data is provided, followed by the fractographic analysis.

219        3.1. Physical state of the samples

220     The fusion bonded samples prepared using the autoclave consolidation process showed non-  
221     uniform thickness, with the centre of the laminates being thicker than the edges. Despite their  
222     thickness (10 mm), the aluminium caul sheets were bent and permanently deformed during  
223     the autoclave cycle as a result of the high pressure applied. In some case, the difference in  
224     thickness between the edge and the centre was up to 0.15 mm. The quality of the samples  
225     manufactured using press consolidation and stamp forming process, in terms of variation in  
226     sample thickness, was superior to the autoclaved samples with the variation in thickness  
227     being always less than 0.05 mm.

228     Typical cross-sectional micrographs for the three fusion bonding techniques and with  
229     different interleave thicknesses are presented in Figure 7. All micrographs showed good  
230     consolidation quality with no voids in the substrates or the interface. For the cases in which a  
231     PEEK film was inserted between the laminates prior to fusion bonding, two different regions  
232     can be distinguished in all the micrographs shown in Figure 7, i.e. a matrix poor region  
233     mainly in the substrates, and a matrix rich region at the bond line. Besides, two different  
234     morphologies can be identified in the matrix rich region. The first is characterised by matrix  
235     material in which many fibres are randomly distributed as shown in the first and second  
236     columns in Figure 7. This morphology arises when fibres migrate, during processing, from  
237     the substrates into the interleaved film at the interface. This happened during the slower  
238     processes, i.e. during autoclave and press consolidation. The second morphology is

239 characterised by matrix material with very few or no fibres. This is evident in the stamp  
240 formed samples (last column in Figure 7), for which there is not enough time for the fibres to  
241 migrate during processing.



242 Figure 7: Cross-sectional micrographs of 6 different specimens close to the interface. Left to right:  
243 autoclave consolidated specimen, press consolidated specimen, and stamp formed specimen. Top row:  
244 specimen interleaved with a 38  $\mu$ m thick film. Bottom row: specimen interleaved with 100  $\mu$ m film in the case of press  
245 consolidation and stamp forming, specimen interleaved with 3 layers of 38  $\mu$ m thick films in the case of  
246 autoclave consolidation. The white bar on the left of the micrograph indicates the thickness of the interleaved  
247 films before processing.

248 The thickness of the matrix rich region was not uniform along the cross-sectional plane for  
249 the autoclaved specimens, which was associated with significant matrix flow during  
250 processing. The effect of this non-uniformity on toughness will be further elaborated in the  
251 next section. On the contrary, the press consolidated, and the stamp formed samples showed a  
252 more uniform thickness of the matrix rich region.

253 3.2. Double cantilever beam experiments

254 This section presents the results of the DCB experiments. First, the issues encountered during  
255 testing are described and examples of force vs. displacement curves are shown. At the end of

256 this section, the results from all the samples tested are combined to generate a plot of fracture  
257 toughness as a function of interleaving thickness.

258         *3.2.1. General observations during DCB testing.*

259 Five DCB specimens were tested for each sample. Nevertheless, several issues were  
260 encountered during DCB testing which made the analysis difficult and reduced the number of  
261 specimens kept for the analysis. The main problems encountered were instability of crack  
262 propagation and the presence of a non-flat resistance curve (toughness vs. crack length). The  
263 former leads to a small number of propagation values, making the specimen less statistically  
264 relevant, while the latter indicates possible variations in crack propagation mechanisms, such  
265 as for example fibre bridging. As both complicate data reduction, two criteria were  
266 implemented to obtain a set of specimen data for analysis. A specimen was kept for analysis  
267 in case it showed i. at least 10 mm of stable crack propagation, and ii. less than 20% variation  
268 in interlaminar toughness along the 10 mm of crack propagation. An exception to the second  
269 criteria was made for the stamp formed specimens. The threshold was changed to 50% in  
270 order to have enough specimens for analysis. It is worth to notice that only few stamp formed  
271 specimens were kept for the analysis which were close to the second criterion. These criteria  
272 led to only three to four consistent specimens from an initial lot of five specimens per sample.  
273 An exception was the sample from the autoclave which was interleaved with three 38 µm  
274 films. Out of the five specimens tested, only two were kept for the analysis. Table 2  
275 summarises the number of specimens discarded and the reason for not using the data. The last  
276 column shows the number of specimens kept for the analysis. From the table, it can be noted  
277 that the standard samples, i.e. the autoclave and press consolidation samples without  
278 interleaving, did not present any problem during testing and all the specimens were kept for  
279 the analysis, while all the samples that were manufactured by a nonconventional procedure,

280 i.e. stamp forming or consolidation with interleaving, showed at least one discarded  
 281 specimen.

Sample Name	Number of specimens			
	Presented at least one point of unstable crack propagation	Did not show at least 10 mm of stable crack propagation	More than 20% or 50% derivation in R-curve	Used for the analysis
<b>Autoclave</b>				
A-None	0	0		5
A-1x38	1	1		4
A-2x38	5	2		3
A-3x38	4	3	0	2
A-4x38	4	1		4
A-5x38	3	1		4
A-6x38	3	2		3
<b>Press</b>				
P-None	0	0	0	5
P-1x38	3	1		4
P-1x100	2	1		4
<b>Stamp</b>				
S-None	2	0	1	4
S-1x38	4	0	1	4
S-1x100	4	0	2	3

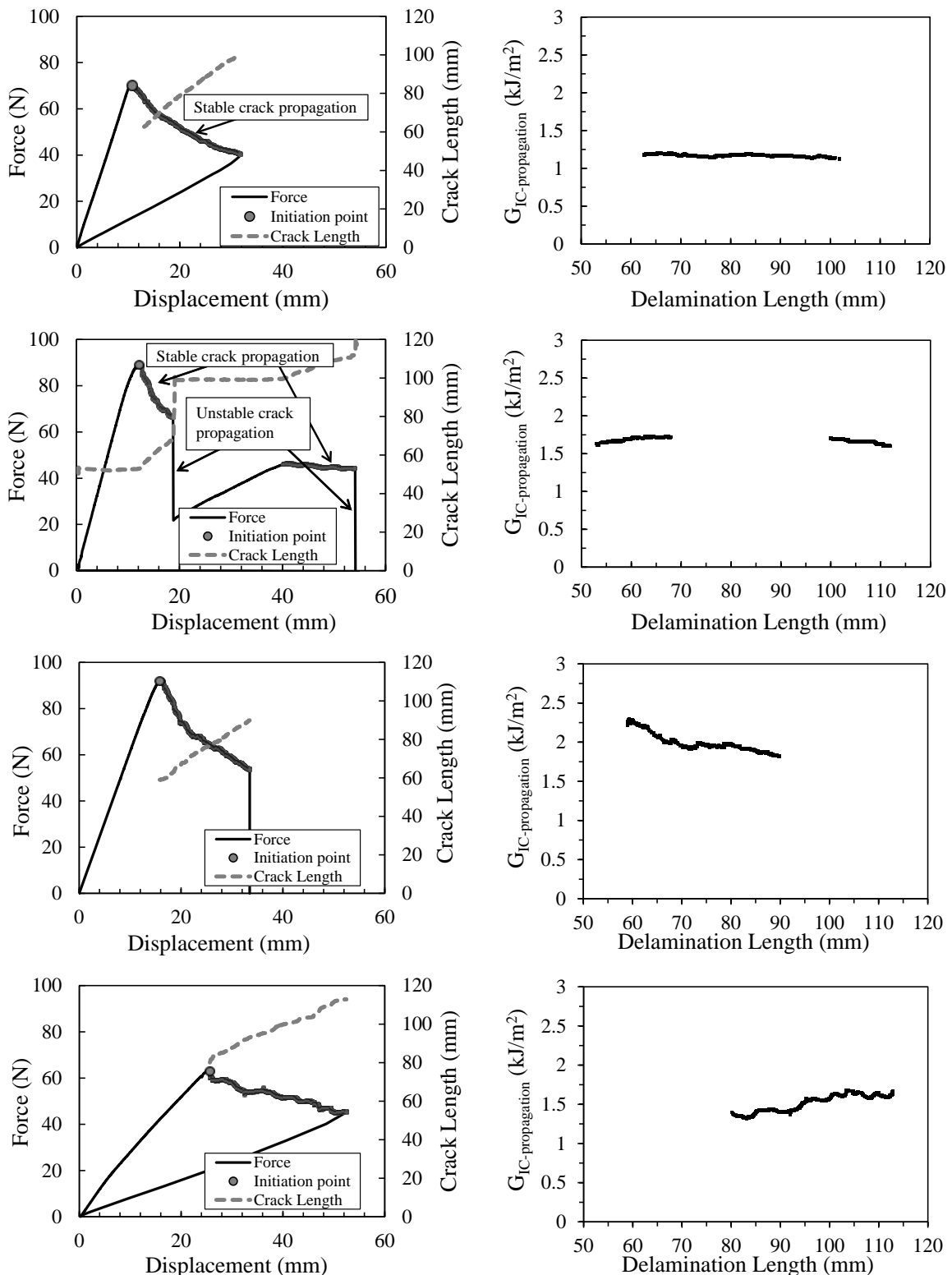
282 Table 2: Overview of the number of specimens discarded and the reason for not using the data. The last  
 283 column shows the number of specimens used for analysis.

284 Two characteristic force - displacement and crack length - displacement curves are shown in  
 285 the upper graphs of Figure 8. The left graph corresponds to a specimen which showed stable  
 286 crack propagation, while the right graph belongs to a specimen which showed a combination  
 287 of stable and unstable crack propagation. During the evaluation of the initiation point, the  
 288 maximum force point occurs almost always before the 5% point. Furthermore, almost no  
 289 residual displacement was observed after the specimens were unloaded. The previous two  
 290 observations means that the material can be analysed according to LEFM by following the  
 291 ISO15024 standard. Fibre bridging was not observed during testing.

292 The R-curves corresponding to the four specimens are shown in the bottom row of Figure 8.  
 293 As shown, only the stable part was used to calculate the interlaminar fracture toughness. The  
 294 first point of the R-curve corresponds to the initiation value for interlaminar fracture

295 toughness. It can be noted that stable crack propagation is correlated with a continuous R-  
296 curve, whereas in the presence of an unstable crack propagation the R-curve is interrupted  
297 and therefore shows separate segments.

298



300 Figure 8: Left column: Force-displacement curve and crack length vs displacement. Right column:  
301 Interlaminar fracture toughness as a function of crack length (R-curves). First row: Press consolidated specimen  
302 that showed only stable crack propagation. Second row: Autoclave specimen that showed a combination of  
303 stable and unstable crack propagation. Third row: Autoclave specimen that showed a descending R-curve.  
304 Fourth row: stamp forming specimen that showed an ascending R-curve.

305 Many of the autoclave consolidated specimens suffered from unstable crack propagation as  
306 was illustrated in Table 2. Moreover, some of the specimens showed non-uniform toughness  
307 along the crack length. In those cases, the trend of the R-curve was mostly decreasing.  
308 Although the press consolidated specimens also suffered from unstable crack propagation,  
309 they showed longer paths of stable crack propagation compared to the autoclave consolidated  
310 samples. Moreover, the R-curves observed in press consolidated specimens were flatter than  
311 the ones observed for the autoclave consolidated samples. Finally, the stamp formed samples  
312 despite several cases of unstable crack propagation showed a long path of stable crack  
313 propagation. Some of these specimens showed a rising R-curve, which in some cases was too  
314 large (more than 50%), leading to the rejection of these specimens for the analysis.  
315 The origin of the unevenness in the R-curves observed in the autoclave and stamp formed  
316 specimens were attributed to two different phenomena. For the case of the Autoclave samples  
317 the decreasing R-curve could be caused by a decreasing interleave thickness towards the end  
318 of the specimen, which is the result of resin outflow during processing. The non-flat R-curves  
319 of stamp-formed specimens may be related to variations in consolidation quality. Although  
320 no voids were observed in the specimens, the degree of healing may vary from place to place.  
321 As the process is highly non-isothermal, it is difficult to control temperature during the  
322 process. However, a complete picture requires an in-depth investigation, which is deemed to  
323 be out of scope of this paper.

### 324           3.2.2. *Fracture toughness vs. interleaved thickness*

325 The results of all the samples tested are summarised in Table 3. An average initiation and  
326 propagation fracture toughness values were calculated for all the samples. The average  
327 initiation value of each sample was calculated by averaging the initiation values of all the  
328 specimens within one sample. The average propagation value per sample was determined by

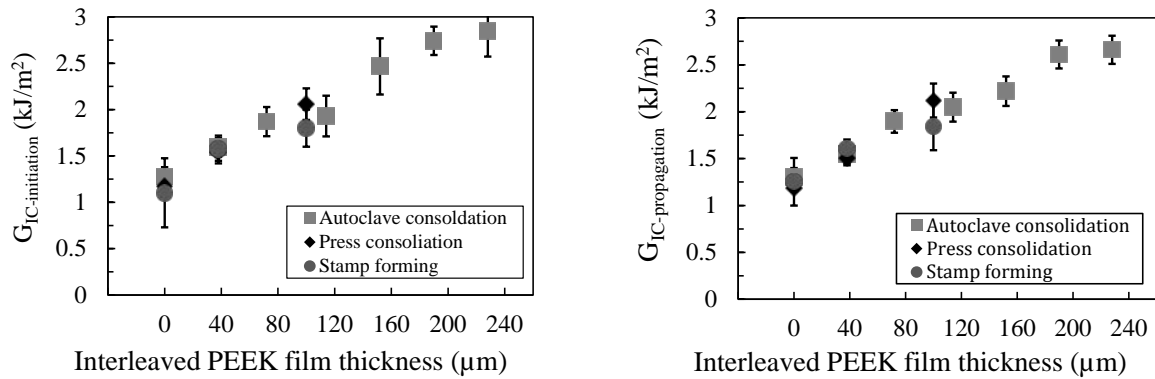
329 averaging the mean propagation value of each specimen within that sample.  
 330 The last column of Table 3 shows the overall trend of the R-curve for each sample, i.e.  
 331 whether the R-curve was observed to be flat (-), ascending (/) or descending (\). It can be seen  
 332 that the trend of the R-curve is closely related to the relation between initiation and  
 333 propagation. In the cases of a flat R-curve the initiation and propagation values are similar,  
 334 whereas with an ascending R-curve initiation values are lower than propagation, and the  
 335 opposite occurs with a descending R-curve.

Sample type, name	Fracture Toughness ( $G_{IC}$ )		R-curve trend
	Initiation (kJ/m <sup>2</sup> )	Propagation (kJ/m <sup>2</sup> )	
<b>Autoclave</b>			
A-None	1.28 ± 0.10	1.30±0.10	-
A-1x38	1.59 ± 0.10	1.55±0.10	-
A-2x38	1.87 ± 0.16	1.89±0.12	-
A-3x38	1.93 ±0.20	2.05±0.16	-
A-4x38	2.46 ±0.30	2.22±0.18	\
A-5x38	2.74 ±0.15	2.61±0.15	\
A-6x38	2.85 ±0.28	2.66±0.20	\
<b>Press</b>			
P-None	1.17±0.10	1.19±0.10	-
P-1x38	1.54±0.10	1.51±0.10	-
P-1x100	2.06±0.17	2.12±0.18	-
<b>Stamp</b>			
S-None	1.10±0.37	1.25±0.25	/
S-1x38	1.57±0.15	1.60±0.10	/
S-1x100	1.80±0.20	1.84±0.25	/

336 Table 3: Fracture toughness values for initiation and propagation for all the sample tested. The error was  
 337 calculated as one standard deviation of the set of values within one sample.

338 Initiation and propagation fracture toughness as a function of the interleaved PEEK film  
 339 thickness is shown in Figure 9 for the three different process technologies used. It is worth  
 340 noticing that the x-axis is the nominal thickness of the added films and not the actual matrix  
 341 rich bond line thickness after processing, which in some cases may be smaller due to outflow  
 342 of matrix. Measurements of the actual matrix rich bond line thickness were difficult to  
 343 perform from the micrograph and therefore not used. The trend is similar for all three  
 344 processes, where the fracture toughness increases with increasing interleave thickness. No

345 significant differences can be observed between the three processes and between initiation  
 346 and propagation. Despite the similar average toughness values, the stamp forming process  
 347 resulted in a higher scatter within the sample. This may be due to a non-uniform pressure and  
 348 temperature distribution during fusion bonding, which may locally have resulted in  
 349 incomplete wetting or healing.

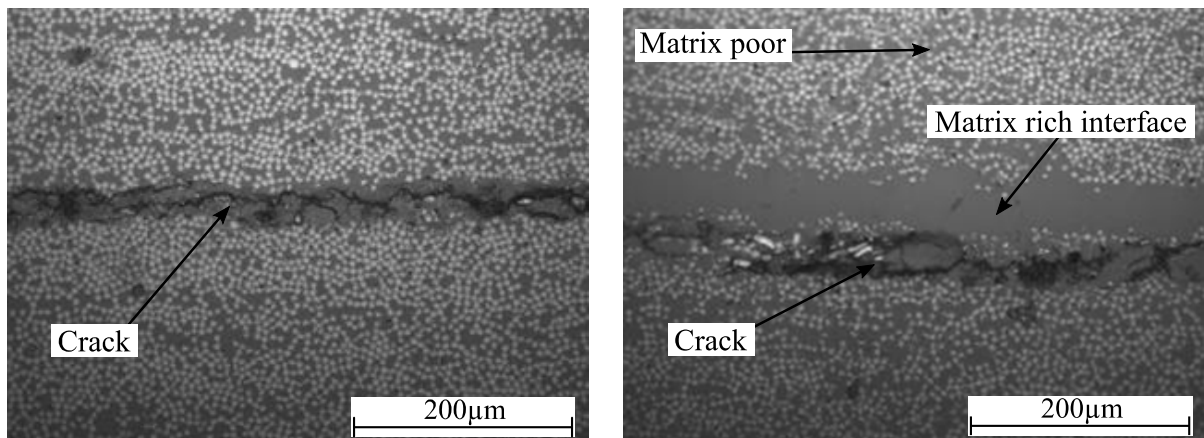


350 Figure 9: Interlaminar fracture toughness as a function of interleaved thickness for the three processes,  
 351 autoclave consolidation, press consolidation, and stamp forming.

### 352 3.3. Fractography

353 The fracture behaviour of the different samples is compared in this section using cross-  
 354 sectional micrographs and fractography analysis. First, a comparison between samples  
 355 without film interleaving and with film interleaving is shown. Later, the comparison between  
 356 samples with fibre migration and without fibre migration is presented. Three types of images  
 357 were used for the analyses. Figure 10 shows cross-sectional micrographs perpendicular to the  
 358 crack propagation direction. These micrographs show the position of the crack at a single  
 359 instant, though they do not give information about how the crack propagates along the length  
 360 of the specimen. Figure 11 shows pictures of the optical cross-sectional micrographs with the  
 361 cross-sectional plane oriented at 20° with respect to the crack propagation direction. These  
 362 pictures show how the crack propagates through the specimen. Finally, Figure 12 shows the  
 363 SEM micrographs of the fracture surfaces where the interaction between fibre and matrix and  
 364 the deformation of the matrix after testing can be observed.

365 The comparison between samples with and without PEEK film interleaving is presented here.  
366 Due to the similarity among the images within each test group, only one representative  
367 micrograph per group is shown. The left micrograph in Figure 10 shows a specimen without  
368 interleaving. It can be seen that the crack is located at the centre plane of the specimen. The  
369 right micrograph shows a specimen with interleaving. In this case, the crack is located close  
370 to the interface between the fibre rich and the matrix rich region, slightly out of the centre of  
371 the specimen. Other images in the same cross-sectional plane, thus to the left or right of the  
372 presented image, showed the same crack at the interface between matrix rich region and the  
373 matrix poor region of the upper substrate.



374 Figure 10: Cross-sectional micrographs perpendicular to the crack propagation direction. Left) autoclave  
375 consolidated specimen without interleaving. Right) stamp formed specimen with interleaving.

376 The straightness of the crack along the propagation direction was analysed using the 20°  
377 cross-sectional micrographs. The top micrograph in Figure 11 shows a non-interleaved  
378 specimen, while the bottom shows an interleaved specimen. It can be noted that the crack  
379 path remains flat when the specimens are not interleaved as is shown in the top. However, the  
380 crack propagates with some waviness, seemingly avoiding the matrix rich region in the  
381 centre, and this is the case for interleaved specimens shown in the bottom image.

382  
383  
384  
385  
386

387  
388  
389

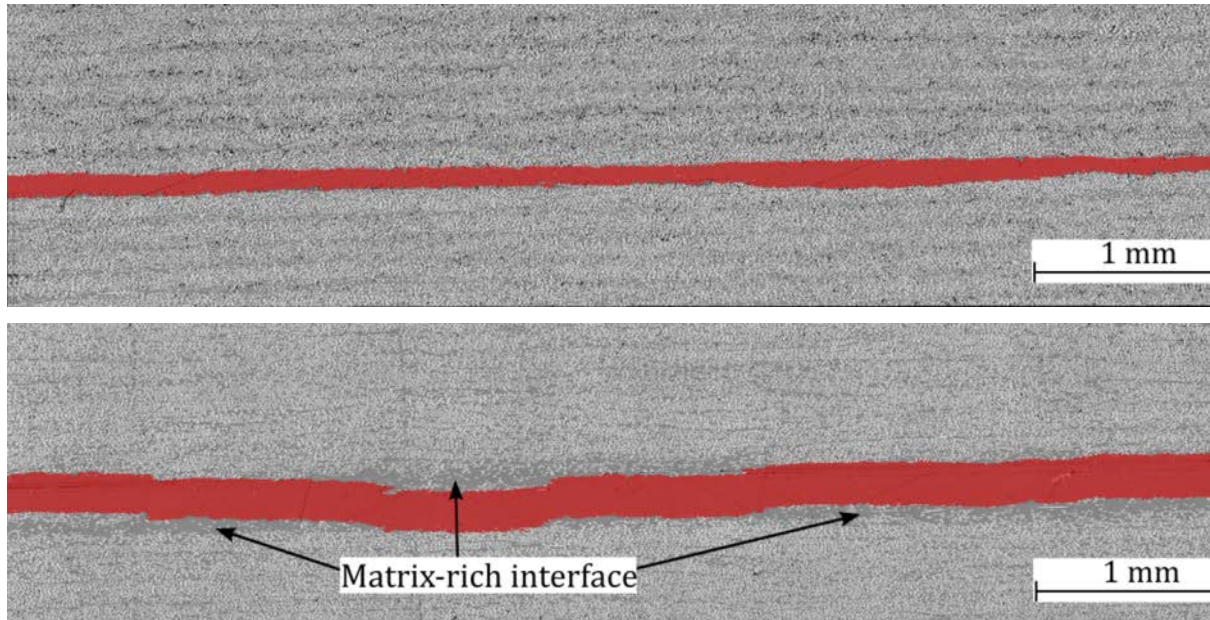
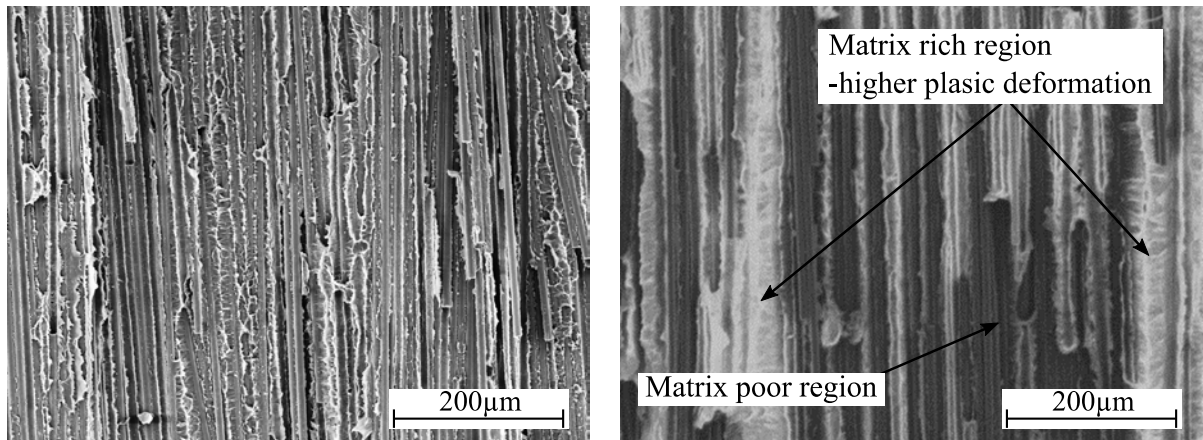
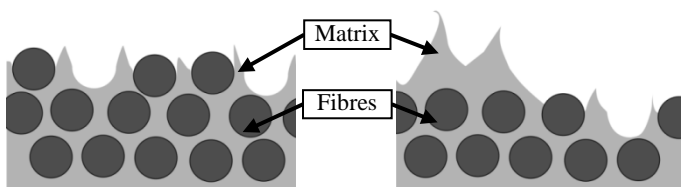


Figure 11: Cross-sectional micrographs were taken at 20° with respect to the crack propagation direction. Top: Non-interleaved stamp formed specimen. Bottom: 100 μ m interleaved press consolidated specimen. The crack is highlighted in red.

393 A comparison between the fracture surface of an interleaved and a non-interleaved specimen  
394 is shown in Figure 12, while Figure 13 shows a schematic illustration of the accompanying  
395 cross-section. The SEM image on the left shows that the fracture surface of a non-interleaved  
396 specimen is characterised by fibre imprints in the matrix and bare fibres. Also, microscale out-  
397 of fracture plane plastic deformation of the matrix can be observed, which is a typical feature  
398 of the fracture surface of carbon/PEEK laminates tested in mode I [23]. This deformation is  
399 present at the edges of the fibres in the schematic view. The SEM micrograph on the right  
400 shows that the fracture surface of an interleaved specimen is characterised by two distinct  
401 regions. The first region shows a combination of fibre imprints in the matrix and bare fibres,  
402 similar to the case of the non-interleaved sample. The second region is characterised by a  
403 matrix rich area where large microscale plastic deformation of the matrix can be observed as  
404 evidenced by the white polymer regions.

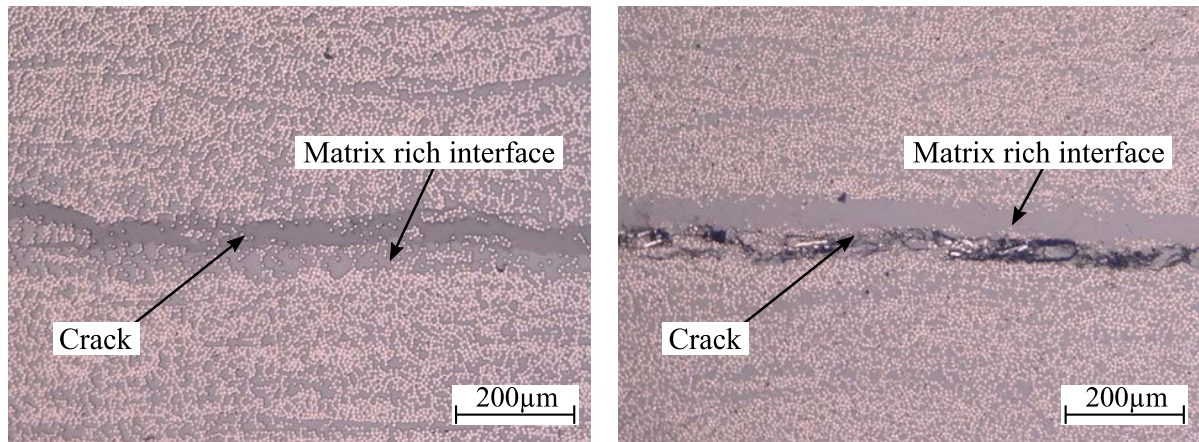


405      Figure 12: Scanning electron micrograph of the fracture surfaces. Left: Autoclave consolidated specimen  
 406      with no interleaving. Right: interleave press consolidated specimen.  
 407

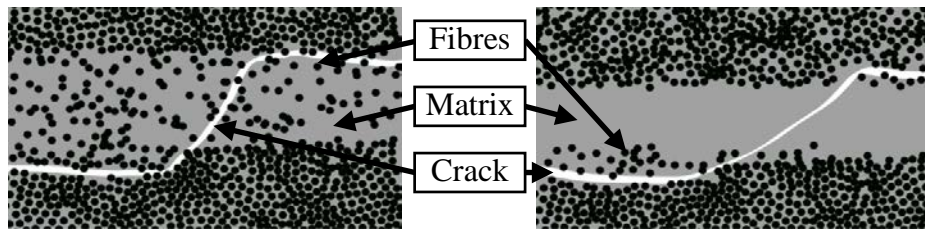


408      Figure 13: Schematic view of a cross-section of a fracture surface. Left: Sample without matrix interleaving.  
 409      Right: Sample with matrix interleaving [Figure 13 near here]

410      The interleaved samples can be subdivided into two groups. The first comprises the samples  
 411      prepared using a slow process (autoclave and press consolidation), while the second group  
 412      consists of samples manufactured using the fast process (stamp forming). Figure 14 and  
 413      Figure 15 show the cross-sectional micrographs and their schematic illustration for both  
 414      groups, respectively. The crack shape and location look similar for both cases, irrespectively  
 415      of whether fibre migration occurred or not. The crack seems to remain at the interface  
 416      between the matrix rich and matrix poor region. The crack path was observed to alternate  
 417      between the top and the bottom substrate trying to minimise the crack path length through the  
 418      matrix rich region, similar to what is observed in Figure 11.



419      Figure 14: Cross-sectional micrographs perpendicular to the crack propagation direction. Left) autoclave  
420      consolidated specimen with interleaving. Right) stamp formed specimen with interleaving.  
421



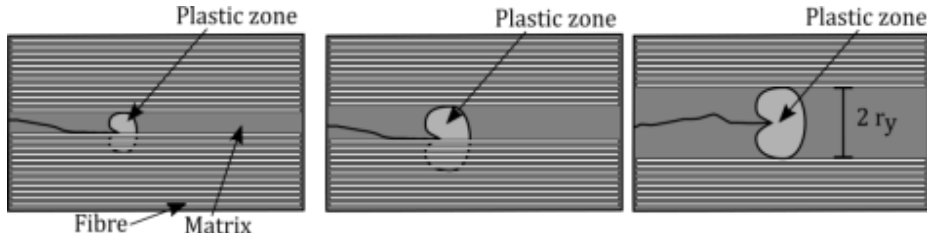
422      Figure 15: Schematic view of a cross-section micrograph of an interleaved specimen. Left: Specimen with  
423      fibre migration as obtained using autoclave or press fusion bonding. Right: Specimen without fibre migration as  
424      obtained using stamp fusion bonding.

#### 425      4. Discussion

426      In this section, the results obtained are combined and discussed with the purpose of getting a  
427      deeper understanding of the mechanisms that govern the interlaminar fracture toughness of  
428      fusion bonded joints that present a matrix rich bond line.

429      The interlaminar fracture toughness improves by increasing the matrix rich bond line  
430      thickness, as was expected. This is true even if the crack does not propagate through the  
431      matrix rich area but through the matrix poor area or the interface between the matrix-poor  
432      (one of the two substrates) and matrix-rich (the interleave) regions. This phenomenon was  
433      explained by Hojo et al. [13] for interleaved laminates, who reasoned that by increasing the  
434      interleave thickness, even if the crack does not propagate fully through the matrix rich area,  
435      the plastic yield zone in front the crack tip is still less constrained by the fibres and is

436 therefore allowed to increase in size. Moreover, it was proposed that when the matrix rich  
 437 region is smaller than the maximum plastic yield zone size, the crack path migrates towards  
 438 the weakest region, i.e. the boundary between matrix poor and matrix rich regions, resulting  
 439 in adhesive failure [13]. However, when the thickness of the matrix rich region increases  
 440 further than the plastic yield zone, the crack will remain within this region resulting in a  
 441 cohesive failure of the interleave [13]. The change in plastic zone size and the position of the  
 442 crack propagation path is schematically represented in Figure 16. A larger plastic yield zone  
 443 area means that more energy will be dissipated, which is reflected by a higher interlaminar  
 444 fracture toughness. The SEM fractography, as presented in Figure 12, confirmed that more  
 445 plastic deformation is observed in the interleaved samples compared to the samples without  
 446 additional matrix at the interface. Besides, the tortuosity of the crack path, as shown in the  
 447 lower micrograph in Figure 11, may also contribute to an increased fracture toughness



448 Figure 16: A schematic explanation of crack growth behaviour and plastic zone development having a radius  
 449  $r_y$ . Left) Base material, no interleaved. Centre) Material with an interleaving thickness below maximum plastic  
 450 yield zone ( $2r_y$ ). Right) Material interleaved with a thickness above the maximum plastic yield zone. Figure  
 451 adapted from [13].

452 Plastic deformation of the matrix was found to be the main mechanism to increase the  
 453 interlaminar fracture toughness of the interleaved specimens. Nevertheless, as the plasticity is  
 454 localised only at the fracture surface, the global linear elastic behaviour of the specimen  
 455 during testing was retained. As such, the tests still comply with the LEFM assumption, which  
 456 makes the comparison of the values obtained for the different samples acceptable.  
 457 It was suggested that the maximum theoretical toughness of an interleaved system is the  
 458 toughness of the pure polymer, which is reached when the interleave thickness is equal or

459 larger than two times the plastic yield radius (Figure 16 right) [16, 18]. A first approximation  
 460 of the plastic zone radius ( $r_y$ ) of a polymer can be calculated following Irwin's plastic zone  
 461 model for plane strain reported by Ozdil and Carlsson [19] (Equation (2)).

$$r_y = \frac{1}{4\pi} \left( \frac{K_{IC}}{\sigma_y} \right)^2 \left( \frac{3}{2} (1 - 2\nu^2) \right), \quad (2)$$

462 where  $K_{IC}$  is the stress intensity factor which relates to the fracture toughness of the polymer,  
 463  $\sigma_y$  is the tensile yield stress of the polymer, and  $\nu$  is the Poisson's ratio. The following  
 464 expression can be used to relate the stress intensity factor  $K_{IC}$  to the energy release rate  $G_{IC}$  in  
 465 case of a plane strain situation:

$$G_{IC} = \frac{(1 - \nu^2) K_{IC}^2}{E}, \quad (3)$$

466 where  $E$  is the elastic modulus of the polymer. Material data from the literature is required to  
 467 calculate the maximum theoretical fracture toughness of this system. The following values  
 468 were reported in the data sheet of Victrex PEEK 150, which is used as matrix in the prepgs;  
 469 tensile yield point ( $\sigma_y$ ) of 105 MPa, an elastic modulus ( $E$ ) of 3.5 GPa and a poisson's ratio  
 470 ( $\nu$ ) of 0.4. The stress intensity factor  $K_{IC}$  for Victrex PEEK 450G, a similar grade of the  
 471 polymer use for interleaving, is reported in literature to lie between  $3$  to  $6$   $\text{MPa}\cdot\text{m}^{1/2}$  [24]. An  
 472 average value of  $4.5$   $\text{MPa}\cdot\text{m}^{1/2}$  will be used for the following analysis. Using Equation (2)  
 473 and Equation (3) a plastic radius of 0.225 mm and an energy release rate of  $4.8$   $\text{kJ/m}^2$  can be  
 474 calculated for this polymer. The result shows that the pure polymer has almost two times  
 475 higher toughness than the interlaminar fracture toughness measured in the experiments in this  
 476 study. Nevertheless, the theoretical matrix rich bond line thickness required to develop the  
 477 fracture toughness (0.45 mm) was not tested in the experiments reported in this work, where  
 478 a maximum matrix rich bond line thickness of 0.2 mm was tested. Thus, the fracture  
 479 toughness is expected to keep increasing by increasing matrix rich bond line thickness.

480 Similar observations were made for thermoset composites [18]. For these material systems,  
481 smaller interleave thicknesses are required to achieve the maximum (i.e. polymer) toughness,  
482 which is caused by the more brittle nature of thermosets compared to thermoplastics.

483 The matrix rich bond line thickness after processing was observed to be not uniform, this is  
484 particularly true for the autoclaved samples where material flow occurs during processing.

485 This non uniformity and the difficulty to distinguish between the matrix rich and matrix poor  
486 region makes it difficult to evaluate the actual matrix rich bond line thickness after  
487 processing. Besides, this non uniformity may, moreover, also be one of the causes for the  
488 unstable crack propagation observed as it most probably resulted in a non-uniform  
489 interlaminar fracture toughness along the crack path. It is known that the unstable crack  
490 propagation may occur when the crack propagates from a region of higher toughness to a  
491 region of lower toughness, as the elastic energy stored in the specimen is more than required  
492 for making the crack to propagate in a stable manner. Or more precisely formulated unstable  
493 crack propagation may occur at the locations where  $dG/da$  exceeds  $dR/da$  [25].

494 The high cooling rates observed during stamp forming may have induced a different level of  
495 crystallinity compared to the other two (slower) processing techniques, possibly affecting the  
496 measured toughness values. DSC experiments showed, however, that a non-interleaved press  
497 consolidated specimens and non-interleaved stamp formed specimens have the same level of  
498 crystallinity of approximately 35% using an enthalpy of crystallisation value of 130 (J/g) [26]  
499 with a matrix weight fraction of 34%. Although the difference in thermal history may have  
500 resulted in different crystal morphologies, this seemed to have no effect on the measured  
501 toughness.

502 In conclusion, it seems that the interlaminar fracture toughness is independent of the three  
503 processes used in this work. It solely depends on the interleave thickness and is not affected  
504 by fibre migration. The amount of fibres, in the fibre migration region, is too small to

505 constrain the plastic zone, nor does it result in excessive fibre bridging.

506 **5. Conclusions**

507 The effect of a matrix rich interface and fibre migration on the fracture toughness of fusion  
508 bonded samples was studied. For this purpose, samples were prepared using manufacturing  
509 technologies having different characteristic processing times, namely: autoclave  
510 consolidation, press consolidation, and stamp forming. Autoclave and press consolidation  
511 were considered as slow processes, while stamp forming was considered as a fast process  
512 with conditions similar to those in many welding techniques. Matrix rich bond lines with  
513 different thicknesses were obtained by interleaving matrix films at the interface between two  
514 adherents prior to fusion bonding.

515 Microscopy showed that two regions can be identified in the interleaved samples, namely the  
516 matrix poor adherent(s) and a matrix rich bond line. The processing time, moreover, affected  
517 the matrix rich bond line morphology. On the one hand, fibre migration from the adherents  
518 into the matrix rich bond lines was observed during (the slower) press and autoclave  
519 consolidation, resulting in a matrix rich zone with many loose fibres. On the other hand, fibre  
520 migration was prevented during (the faster) press forming, resulting in a bond line with very  
521 few or no fibres. Double cantilever beam experiments were performed and showed that the  
522 increase in the matrix rich bond line improves the fracture toughness. This increase is  
523 attributed to the development of microscale matrix plastic deformation. Moreover, it was  
524 shown that fibre migration has a negligible effect on the interlaminar fracture toughness, i.e.  
525 the toughness only depends on the matrix interleave thickness.

526 **6. Acknowledgements**

527 The authors gratefully acknowledge the financial as well as technical support from the  
528 industrial and academic members of the ThermoPlastic composites Research Center (TPRC)

529 as well as the support funding from the Province of Overijssel for improving the regional  
530 knowledge position within the Technology Base Twente initiative.

531 **7. Reference**

532

- [1] A. Benater and T. G. Gutowski, "Methods for fusion bonding thermoplastic composites," *SAMPE Quarterly*, vol. 18(1), pp. 35-42, 1986.
- [2] A. P. da Costa and et al., "A review of welding technologies or thermoplastic composites in aerospace applications," *Journal of Aerospace Technology and Management*, vol. 4.3, pp. 255-266, 2012.
- [3] P. Davies and et al., "Joining and repair of a carbon fibre-reinforced thermoplastic..," *Composites*, vol. 22.6, pp. 425-431, 1991.
- [4] S. M. Todd, "Joining Thermoplastic Composite.," *Proceedings of the 22nd International SAMPE Technical Conference*, vol. 22, pp. 383-392, 1990.
- [5] A. Yousefpour, M. Hojjati and J. Immarigeon, "Fusion bonding/welding of thermoplastic composites," *Journal of Thermoplastic Composite Materials*, vol. 17(4), pp. 303-341, 2004.
- [6] M. M. Schwartz, "Joining of composite-matrix materials," *Materials Park - ASM International*, 1994.
- [7] I. Da Baere, K. Allaer, S. Jacques, W. Van Paepegem and J. Degrieck, "Interlaminar behavior of infrared welded joints of carbon fabric-reinforced polyphenylene sulfide.," *Polymer Composites*, vol. 33, pp. 1105-1113, 2012.
- [8] W. J. Cantwell and et al., "Thermal joining of carbon fibre reinforced PEEK laminates.," *Composite Structures*, vol. 16.4, pp. 305-321, 1990.
- [9] J. C. Fish and et al., "Interlaminar fracture characteristics of bonding concepts for thermoplastic primary structures.," *AIAA journal*, vol. 30.6, pp. 1602-1608, 1992.
- [10] C. Ageorges, L. Ye and M. Hou, "Advances in fusion bonding techniques for joining thermoplastic matrix composites: A review.," *Composites - Part A: Applied Science and Manufacturing*, vol. 32(6), pp. 839-857, 2001.
- [11] R. Fracasso, M. Rink, A. Pavan and R. Frassine, "Effects of strain-rate and temperature on the interlaminar fracture toughness of interleaved PEEK/CF composites.," *Composites Science and Technology*, vol. 61(1), pp. 57-63, 2001.
- [12] O. Ishai, H. Rosenthal, N. Sela and E. Drukker, "Effect of selective adhesive interleaving on interlaminar fracture toughness of graphite/epoxy composite laminates," *Composites*, vol. 19(1), pp. 49-54, 1988.
- [13] M. Hojo, T. Ando, M. Tanaka, T. Adachi, S. Ochiai and Y. Endo, "Modes I and II interlaminar fracture toughness and fatigue delamination of CF/epoxy laminates with self-same epoxy interleaf.," *International Journal of Fatigue*, 2006.
- [14] K. Shivakumar and R. Panduraga, "Interleaved polymer matrix composites - A review.," *54th AIAA/ASME/ASCE/AHS/ASC Structures, Structural Dynamics, and Materials Conference*, 2013.
- [15] S. F. Chen and B. Z. Jang, "Fracture behaviour of interleaved fiber-resin composites." 41.1 (1991): 77-97, "Composites Science and Technology", vol. 41.1, pp. 77-97, 1991.
- [16] A. J. Kinloch and S. J. Shaw, "The fracture resistance of a toughened epoxy adhesive," *The Journal of Adhesion*, vol. 12(1), pp. 59-77, 1981.
- [17] M. D. Banea, L. F. Da Silva and R. D. Campilho, "The effect of adhesive thickness on the mechanical behavior of a structural polyurethane adhesive.," *The Journal of Adhesion*, vol. 91.5, pp. 331-346, 2015.
- [18] S. Singh and I. K. Patridge, "Mixed-mode fracture in an interleaved carbon-fibre/epoxy composite.," *Compos Sci Technol*, vol. 55, pp. 319-327, 1995.
- [19] F. Ozdil and L. A. Carlsson, "Plastic zone estimates in mode I interlaminar fracture of interleaved composites.," *Engineering Fracture Mechanics*, vol. 41(5), pp. 645-658, 1992.
- [20] W. S. Jojno and P. D. Mangalgiri, "Investigation of fiber bridging in double cantilever beam specimens," *Journal of Composites Technology and Research*, vol. 9(1), p. 10, 1987.
- [21] G. B. Murri, "Effect of data reduction and fiber-bridging on Mode I delamination characterization of

- unidirectional composites," *Journal of Composite Materials*, vol. 48.19, pp. 2413-2424, 2014.
- [22] "ISO 15114- Fibre-reinforced plastic composites - Determination of the mode II fracture resistance for unidirectionally reinforced materials using the calibrated end-loaded split (C-ELS) test and an effective crack length approach," 2014.
- [23] D. Purslow, "Matrix fractography of fibre-reinforced thermoplastics, Part 1. Peel failures," *Composites*, pp. 365-374, 1987.
- [24] R. Gensler, p. Béguelin, C. J. Plummer, H. Kausch and H. Münstedt, "Tensile behaviour and fracture toughness of poly(ether ether ketone)/poly(ether imide) blends.," *Polymer Bulletin*, vol. 37(1), pp. 111-118, 1996.
- [25] T. W. Aifantis and E. C. Webb, "Crack growth resistance curves and stick-slip fracture instabilities," *Mechanics Research Communications*, vol. 24, pp. 123-130, 1997.
- [26] A. A. Mehmet-Alkan and J. N. Hay, "The crystallinity of PEEK composites," *Polymer*, vol. 34(16), pp. 3529-3531, 1993.